Waste Management 187 (2024) 262–274

Contents lists available at ScienceDirect

Waste Management

journal homepage: www.elsevier.com/locate/wasman

Research Paper

Reuse potential of municipal solid waste incinerator bottom ash as secondary aggregate: Material characteristics, persistent organic pollutant content and effects of pH and selected environmental lixiviants on leaching behaviour

Felipe E. Sepúlveda Olea [a,*], Ian T. Burke [b], Arif Mohammad [c], Douglas I. Stewart [a]

[a] School of Civil Engineering, University of Leeds, Leeds LS2 9JT, UK
[b] School of Earth and Environment, University of Leeds, Leeds LS2 9JT, UK
[c] Geoenvironmental Research Centre, Cardiff University, Cardiff CF24 3AA, UK

ARTICLE INFO

Keywords:
MSW IBA
Metal leaching
Persistent organic pollutants
Circular economy
Environmental lixiviants

ABSTRACT

Increasing municipal solid waste (MSW) production poses challenges for sustainable urban development. Modern energy-from-waste (EfW) facilities incinerate MSW, reducing mass and recovering energy. In the UK, MSW incineration bottom ash (MSW IBA) is primarily reused in civil engineering applications. This study characterizes UK-produced MSW IBA, examining its pH-dependent leaching behaviour and response to environmental lixiviants. Results show predominant components include a melt phase, primary glass and fine ash aggregations, and a chemical composition dominated by SiO_2 (30–50 %), CaO (~15 %), Fe_2O_3 (~10 %), and Al_2O_3 (~8%). X-ray absorption near edge structure (XANES) analysis shows that Zn and Cu are most likely oxygen-bound (adsorbed to oxy-hydroxides and as oxides) with some sulphur bound. Polychlorinated biphenyls (PCBs) and polychlorinated dibenzodioxins/furans (PCDD/Fs) are well below regulatory limits, and polycyclic aromatic hydrocarbons (PAHs) were undetectable. Leaching tests indicate trace elements mobilize at pHs $\leq$ 6. With a natural pH of 11.3 and high buffering capacity, significant acid inputs to the MSW IBA are required to reach this pH, which are improbable in the environment. Wood chip additions increase leachate's dissolved organic carbon (DOC) and reduce pH, but had minimal impact on metal-leaching behaviour. Synthetic plant exudate solutions minimally affect metal leaching at realistic concentrations, only enhancing leaching at $\geq$ 1500 mg l^{-1} DOC. This work supports MSW IBA's low-risk in specified civil engineering applications.

1. Introduction

Continued growth of municipal solid waste (MSW) production (2000 Mt $year^{-1}$ produced globally in 2016 as compared to 635 Mt $year^{-1}$ in 1965 (Chen et al., 2020; Kaza et al., 2018; Shah et al., 2021)) has made its management an increasingly important challenge to the sustainable development of most cities (Zhu et al., 2020; Loginova et al., 2019; Shah et al., 2021). Therefore, incineration of MSW at modern energy from waste (EfW) facilities is increasingly used to treat residual MSW, reducing its mass and volume, removing biodegradable materials, and providing an opportunity to recover energy (Zhang et al., 2010; Shah et al., 2021). The World Bank reported in 2018 (Kaza et al., 2018) that

Abbreviation: ads, adsorbed; DOC, dissolved organic carbon; EC, electrical conductivity; EfW, energy from waste; EU, European Union; GC–MS, gas chromatography – mass spectrometry; HFO, hydrous ferric oxide; HRGC-HRMS, high resolution gas chromatography- high resolution mass spectrometry; ICP-OES, inductively coupled plasma – optical emission spectrometry; LCF, linear combination fitting; L/S, liquid/solid ratio; MSW, municipal solid waste; MSW IBA, municipal solid waste incineration bottom ash; PAHs, polycyclic aromatic hydrocarbons; PCBs, polychlorinated biphenyls; PCDD/Fs, polychlorinated dibenzodioxins/furans; POPs, persistent organic pollutants; PSD, particle size distribution; PTEs, potentially toxic elements; SEM-EDX, scanning electron microscopy and energy dispersive X-ray spectroscopy; TEF, toxic equivalent factors; TEQ, toxic equivalent; UK, United Kingdom; US EPA, United States Environmental Protection Agency; XANES, X-ray absorption near edge structure; XRD, X-ray diffraction; XRF, X-ray fluorescence.

* Corresponding author.
E-mail addresses: f.sepulvedaolea@leeds.ac.uk (F.E. Sepúlveda Olea), i.t.burke@leeds.ac.uk (I.T. Burke), mohammada2@cardiff.ac.uk (A. Mohammad), d.i.stewart@leeds.ac.uk (D.I. Stewart).

https://doi.org/10.1016/j.wasman.2024.07.026
Received 12 April 2024; Received in revised form 14 June 2024; Accepted 21 July 2024
Available online 29 July 2024

globally 11 % of MSW was disposed of via incineration, while this percentage was 22 % in high-income countries, where this management method is primarily used.

MSW incineration typically results in 75–80 % mass and 90 % volume reduction. MSW incineration bottom ash (IBA) is the major solid residue from incineration (80 wt%), with fly ash/ air pollution control residues making up the balance (Blasenbauer et al., 2020; Loginova et al., 2019; Brunner and Rechberger, 2015; Morf et al., 2000). IBA is a complex, mostly inorganic material composed of a mineral fraction (80–85 wt%, including melt components, synthetic ceramics, stones and fine materials), metals (ferrous 7–10 wt% and non-ferrous 1–5 wt%) and a minor fraction of unburned material (<1 wt%) (Blasenbauer et al., 2020; Wei et al., 2011; CEWEP, 2016; Chandler et al., 1997; Chimenos et al., 1999; Holm and Simon, 2017; Huber et al., 2020; Aubert et al., 2006). Due to their economic value, around 85–95 wt% of the ferrous metals and 40–65 wt% of the non-ferrous metals are typically recovered and subsequently recycled in the metal industry (Blasenbauer et al., 2020). Whilst metal recovery is a common practice, the fate of the residual fraction varies with the local regulatory environment (Loginova et al., 2019; Blasenbauer et al., 2020). Where it occurs, reuse of MSW IBA is principally as a secondary raw material in the civil engineering sector (e.g. road construction, earthworks, cement process and bound or unbound in foundations) (Blasenbauer et al., 2020; Loginova et al., 2019; Zhu et al., 2020; Forteza et al., 2004; Lam et al., 2010).

Together the EU, Norway and Switzerland generated about, 17.6 Mt of IBA annually between 2015 and 2019 (Blasenbauer et al., 2020). Reuse is permitted in these countries if the quantities of potentially toxic elements (PTEs) and salts are below mandatory thresholds (Loginova et al., 2019; Blasenbauer et al., 2020). Unfortunately, there are no harmonised limit values at EU level and individual countries have developed their own regulations for the reuse of IBA. As a result, these regulations vary significantly between countries, with some countries setting limits on the total content of PTEs whereas others limit the leachable content (Blasenbauer et al., 2020). Further, the methodology to determine leachable content of PTEs (i.e. leaching tests protocols) also vary between countries (Blasenbauer et al., 2020; Van Gerven et al., 2005; Crillesen and Skaarup, 2006). However, between 2015 and 2019, about half of the IBA produced in EU, Norway and Switzerland was utilised outside of landfills (Blasenbauer et al., 2020).

In the UK there were 53 MSW incineration plants in 2021, which processed 14.9 Mt of MSW that year, with an output of 19.8 % of that tonnage as IBA (Tolvik, 2022). This made the UK the third largest producer of IBA in Europe in 2021, after Germany and France (Tolvik, 2022; Blasenbauer et al., 2020; Lederer et al., 2018). The UK regulations on the reuse of MSW IBA (UKEA, 2023) do not specify maximum elemental concentrations for PTEs, and instead refer to the UK "Guidance on the classification and assessment of waste" (Blasenbauer et al., 2020; UKEA, 2023; UKEA, 2021; Lewin et al., 2012). These regulations require that MSW IBA is assessed against a number of "hazard properties", and classify it as non-hazardous or hazardous depending on whether the overall concentrations of "dangerous substances", such as compounds containing PTEs, exceed prescribed limits. 99 wt% of the UK MSW IBA, regulated by this guidance, is re-used for specified construction activities (Blasenbauer et al., 2020).

The UK approach requires data on PTE speciation, otherwise assuming a precautionary worse-case scenario (UKEA, 2021; Lewin et al., 2012), but the majority of European countries base their legislation on leachability of PTEs (Loginova et al., 2019; Blasenbauer et al., 2020; Zhu et al., 2020; van den Berg and West, 1997). Neither of these approaches, however, consider all relevant environmental conditions, such as the presence of environmental lixiviants (such as plant derived organic compounds), which may cause increased release of PTEs from MSW IBA into soils and surface or groundwater, producing potential effects of human toxicity and eco-toxicity (Zhu et al., 2020; Yao et al., 2010; Kong et al., 2016; Funari et al., 2019; Jadhav et al., 2018). Furthermore, little attention has been placed on the content of persistent organic pollutants (POPs) of MSW IBA, and whether these may be present at concentrations that pose a risk for re-use.

This study characterized a UK produced MSW IBA (composition, mineralogy and particle size distribution). Polychlorinated biphenyls (PCB), polychlorinated dibenzodioxins/furans (PCDD/Fs) and polycyclic aromatic hydrocarbons (PAH) contents were determined (the POPs of most concern). The speciation of main PTEs (Zn and Cu) was determined by x-ray absorption near edge spectroscopy (XANES). The leachability of PTEs was assessed in batch leaching tests at pH2-12, and compared to available European guidelines for PTE leaching. The effect that organic environmental lixiviants have on the PTE concentrations leaching from the MSW IBA was studied using wood chips and a synthetic plant root exudate solution, which represent common sources of metal binding organic ligands in the environment. Finally, the environmental implications of using unbound MSW IBA in construction under different environmental conditions are discussed.

2. Material and methods

2.1. MSW incineration bottom ash samples

Three MSW IBA samples were collected from an EfW facility in the North-East of England. This plant primarily processes residual household waste with some commercial waste using conventional moving grate combustion technology (UK regulations require combustion gas temperature to exceed 850 °C, but the typical operating temperature of an EfW incinerator is around 1000 °C (Smith and Sutherland, 2022; Suez, n.d.; UKEA, 2009)) and a wet extraction system. Metals are recovered from dry IBA by magnetic and eddy current separation. The samples were taken from stockpiles of materials that will meet the UK Standards for Highways as "selected granular fill" types 6F and 6N after blending (HA, 2022). One sample was collected from a stockpile of material screened by the plant to contain particles predominantly in the range 14 to 45 mm screen (here on referred to as coarse MSW IBA, Fig. S.3). Two further samples were collected from different sections of a second stockpile of material screened by the plant to contain particles predominantly below < 14 mm (here referred to as medium MSW IBA [Fig. S.2] and fine MSW IBA [Fig. S.1] based on particle size analysis contained herein; see Section 3.1 below). Samples were collected immediately after production, and stored in sealed plastic containers for 4 years.

2.2. Particle size distribution

The coarse MSW IBA sample was divided by coning and quartering into ~ 2 kg subsamples, while the medium and fine MSW IBA samples were divided using a riffle splitter into ~ 500 g and ~ 250 g subsamples. The particle size distribution (PSD) of 3 subsamples per sample was determined by sieving (Geoengineer.org; BSI, 2022; Head, 1980).

2.3. Compositional and mineralogical characterization of MSW IBA

XRF, XRD and XANES were conducted on subsamples of the medium MSW IBA, fine MSW IBA, and a composite sample of particles < 1.18 mm from both the medium and fine MSW IBA (named < 1.18 mm fraction), that were milled to < 75 μm (Vibratory Disc Mill RS 200).

2.3.1. Macroscopic description and classification of ash components

Macroscopic visual classification of the particles > 2 mm was carried out on 1 kg sub-samples that were sieved to remove finer particles. The material was washed with distilled water to remove any coating of fines on particle surfaces and allowed to dry, and where necessary, particles were fractured to expose a surface for identification. Each particle was observed with a 14x Hastings Triplet Magnifier (Bausch & Lomb) and classified into one of nine categories. These were primary glass, secondary glass, metals, tiles, other ceramics (crockery), other ceramics

(construction), aggregations, others (rock, minerals, char) and fines.

2.3.2. X-ray fluorescence (XRF) spectroscopy

XRF analysis was carried out using a Rigaku ZSX Primus II spectrometer on triplicate samples prepared as fused beads (major elements) and pressed pellets (trace elements) (see SI Section S.1.A).

2.3.3. X-ray diffraction (XRD) analysis

Mineralogical analysis was undertaken in triplicate on 50 − 100 mg of milled sample mounted on silicon slides on a Bruker D8 X-ray diffractometer using Cu Kα radiation and scanning between 2°and 70° 2θ. Qualitative characterization was carried in all samples, but semi-quantitative analysis was made only on the fine MSW IBA and < 1.18 mm fraction samples as they had a lower component of amorphous phases. The software TOPAS (Total Pattern Analysis Solution- Bruker) was used for semi-quantitative analysis.

2.3.4. Scanning electron microscopy and energy dispersive X-ray spectroscopy (SEM-EDX)

In order to determine the association of specific elements with different phases present in the MSW IBA, SEM-EDX analysis was carried out on five MSW IBA polished sections, prepared from various size fractions. Ash samples were set in epoxy resin (Huntsman Advanced Materials) to form a resin block that was subsequently polished using 3-, 1- and 0.25 − μm diamond paste (Struers) and water-free lubricants. Backscatter electron micrographs and elemental maps were obtain using a Tescan VEGA3 XM equipped with an Oxford instruments X-max 150 SDD EDX using Aztec 3.3 software. A beam energy of 15 keV was used, at a 15 mm working distance and elemental mapping was performed at a resolution of 2 μm.

2.3.5. X-ray absorption near edge spectroscopy (XANES)

To determine the most likely PTE containing phases, Cu K-edge (8979 eV) and Zn K-edge (9659 eV) XANES spectra were collected from milled samples of MSW IBA (medium, fine and < 1.18 mm fraction) on station I18 at the Diamond Light Source, UK. Samples were prepared as 8 mm powder pellets held in Kapton™ tape. Data collection was performed at room temperature (~295 °K) within a He-filled bag. A range of Cu and Zn containing chemicals, natural minerals and solutions were used as standard reference materials (see SI Section S.1.B and Table S.1).

Scans from different locations were averaged to improve the signal to noise ratio using Athena version 0.9.26 (Ravel and Newville, 2005). Spectra were corrected for any drift in E_0 using the data collected from the metal foil standards. Linear combination fitting (LCF) was performed in Athena using the full range of available standards to determine the most likely combinations of standards to best fit the sample. In the final LCF analysis the number of standards used was limited to a maximum of 3 to reduce the degree of freedom present. LCF typically produced results of elemental speciation with an uncertainty of ± 4 %.

2.3.6. Analysis of persistent organic pollutants (POPs)

Five replicates of the fine MSW IBA were analysed for PCDDs/PCDFs (17 congeners), PCBs (12 congeners) and PAHs (EPA 16) by a commercial laboratory (NWG Scientific services, Tyne & Wear, UK). Samples for PCDD/PCDF analysis were extracted and analysed using a method based on US EPA Method 1613 (USEPA, 1994) and those for PCB analysis by US EPA Method 1668 (USEPA, 2010) (modified methods are accredited under the UKAS accreditation scheme). In both cases samples were soxhlet extracted and analysed by high resolution gas chromatography- high resolution mass spectrometry (HRGC-HRMS) (details in SI Section S.1.C). PAHs contents were determined by mixing the samples with sodium sulphate, extraction with dichloromethane and analysis by gas chromatography – mass spectrometry (GC–MS) in SIM (selected ion monitoring) mode.

PCDD/PCDF and PCB results are reported as toxic equivalent (TEQ), which consists in recalculating the concentration of each congener using their respective toxic equivalent factors (TEF), which indicates how toxic they are in comparison with 2,3,7,8-TCDD, the most potent dioxin. Individual congener TEQs are then added to obtain a total TEQ for PCDDs/PCDFs and PCBs.

2.4. pH dependant batch leaching tests

Batch leaching tests based on the US EPA Leaching Environmental Assessment Framework (LEAF) and US EPA method 1313 (Kosson et al., 2017; USEPA, 2017) were performed on the fine MSW IBA. Triplicate samples (20 g dry weight) were placed in 250 ml Nalgene™ bottles (the moisture content of each ash fraction was determined in triplicate so the dry weight could be calculated), and deionised water or HNO_3 with concentrations of up to 1 M was added at a liquid/solid (L/S) ratio of 10. The bottles were then placed on a roller mixer for 72 hrs at room temperature. The final pH and electrical conductivity (EC) of the solution were measured (HACH HQ40D pH meter with HACH Intellical pH and EC probes), and an aliquot of solution was syringe filtered (0.45 μm) for metal analysis by inductively coupled plasma − optical emission spectrometry (ICP-OES) (Thermo Scientific iCAP 7400 Radial). Blank bottles with Milli-Q water alone and Milli-Q water with the maximum HNO_3 concentration were included for quality control.

2.5. Leaching tests with environmental lixiviants

Leaching tests with the synthetic exudate solutions were carried out using the same procedure as the pH dependant batch leaching tests but using a synthetic exudate solution instead of HNO_3. The synthetic exudate solution was developed by Lu et al (2017) and contained 150 mM glucose, 25 mM acetate, 25 mM citrate, 25 mM formate and 37.5 mM serine. Triplicate leaching tests were conducted with the full strength solution and with 5 different dilutions, that contained 14,000 (full strength), 9000, 5000, 1500, 500 and 50 mg l^{-1} of DOC, respectively. This last dilution approximates to soil solutions found in the environment (Lu et al., 2017).

Similarly, triplicate water leaching tests were performed on mixtures of ash (20 g dry weight) and wood chips (either 1, 2, 3, 4 or 5 g dry weight), using chipped (<4 mm), young, freshly felled Norway Spruce (*Picea abies*) from a forested area in West Yorkshire (UK). Milli-Q water was added at a L/S ratio of 10 based on the combined dry weight of ash and wood chips.

Dissolved organic carbon (DOC) was analysed in the collected supernatant with an Analytik Jena Multi N/C 2100 combustion analysers calibrated using commercially prepared stocks of organic and inorganic carbon.

2.6. PHREEQC modelling

The geochemical model PHREEQc (Phreeqc Interactive 3.7.3) (Parkhurst and Appelo, 2013) was used to simulate the acid neutralization of MSW IBA. Two scenarios were modeled, one only considering mineral dissolution and a second one considering both dissolution and surface complexation. The dissolution of mineral phases was simulated based on the minerals determined by XRD, and the mineral parameters were obtained from the Lawrence Livermore National Laboratory (LLNL, n. d.). The surface complexation model was developed using Fe(hydr)oxides (HFO) as a model phase, with a surface area of 600 m^2g^{-1} (Dzombak and Morel, 1991). Two types of sorption sites were used: weak (0.2 mol mol-Fe^{-1}) and strong (0.005 mol mol-Fe^{-1}). To simplify the model, the available surface was considered constant and the dissolution of Fe (hydr)oxides was ignored.

2.7. Statistics

Statistical analysis was carried out in Microsoft Excel (2016) using the data analysis package.

3. Results

3.1. Characteristics of the MSW incineration bottom ash

3.1.1. Particle size distribution

Sieve analysis showed that the coarse MSW IBA is a uniformly graded gravel ($C_u = 1.5$ and $C_c = 1.1$), the medium MSW IBA is a poorly (to well) graded gravel ($C_u = 5.7$ and $C_c = 2.8$), and the fine MSW IBA is a medium graded sandy gravel ($C_u = 6.8$ and $C_c = 0.8$) (ISO, 2017) (SI Figure S.4 and Table S.2). The d_{50} values of the coarse, medium and fine fractions were 16.7, 9.7, 1.8 mm, respectively (50 wt% of the sample is finer than this size). Fine particles (<1.18 mm) constituted ~ 0, 7.2 and 27.0 % of the coarse, medium and fine MSW IBA respectively.

3.1.2. Main components in MSW IBA identified by visual description (>2mm fraction)

The predominant particle type was a melt phase formed during the incineration process (secondary glass, 36.4 wt%), identified by its porosity (gas bubbles), vesicles, cracks and inclusions of other materials (del Valle-Zermeño et al., 2017; Speiser et al., 2001). The second most abundant particle type was fragments of bottles and other glass items (primary glass, 27.4 wt%). The remaining particle were tiles and ceramics, metal fragments, aggregations (constituted mainly by fine ash and occasional fragments of glass, ceramics and metals) as well as some rocks and char (SI Figure S.5).

3.1.3. Chemical composition of MSW IBA

Si was the most abundant element in MSW IBA (Table 1), with higher concentrations in the medium MSW IBA, and lowest in the < 1.18 mm fraction. Ca was the second most abundant element, but with the opposite trend of increasing concentrations in samples with smaller particle sizes. Fe and Al follow in order of abundance. While Fe does not show a systematic variation with particle size, Al concentration increased with decreasing particle size. Na was the fifth most abundant element, and like Si its concentration decreased in samples with smaller particle sizes.

Zn was the most abundant PTE in the IBA samples, and its concentration increased in samples with smaller particle sizes (Table 2). Other PTEs all also have higher concentrations in samples with smaller particle sizes, with concentrations averaged across the IBA fractions decreasing in the order Cu (second most abundant), Cr, Pb, Sn, Ni and Mo.

3.1.4. Mineralogy of MSW IBA

The medium MSW IBA, fine MSW IBA, and the < 1.18 mm fraction all contained the same mineral phases (SI Figure S.6), in order of abundance (measured in fine and < 1.18 mm MSW IBA) quartz (~50 %) > microcline and calcite (10–20 %) > ettringite (5–10 %) > hematite, magnetite and albite (0.3–2 %) (details in SI Table S.3). Primary and secondary glass as amorphous phases do not produce an XRD peak pattern, but their prevalence as main components may account for the elevated background signal that was seen particularly in XRD spectra of the medium MSW IBA between 15 and 40° 2θ.

Table 1
Average concentration of major element oxides by fusion (XRF) reported as mean ± the confidence interval (t-distribution) of 3 replicates.

Wt%	Medium MSW IBA	Fine MSW IBA	<1.18 mm fraction
SiO_2	49.9 ± 0.5	38.0 ± 0.4	29.1 ± 2.2
CaO	13.60 ± 0.03	16.2 ± 0.1	17.4 ± 1.2
Fe_2O_3	9.3 ± 0.1	10.5 ± 0.1	7.9 ± 0.4
Al_2O_3	6.98 ± 0.01	8.80 ± 0.05	14.4 ± 1.1
Na_2O	6.4 ± 0.1	3.96 ± 0.07	2.1 ± 0.2
MgO	1.58 ± 0.01	1.93 ± 0.01	1.8 ± 0.1
K_2O	0.95 ± 0.01	0.99 ± 0.01	0.98 ± 0.06
TiO_2	0.62 ± 0.01	1.03 ± 0.01	1.24 ± 0.09
P_2O_5	0.71 ± 0.01	1.16 ± 0.01	1.4 ± 0.1
MnO	0.12 ± 0.00	0.17 ± 0.00	0.21 ± 0.01
LOI (1025 °C)	6.2 ± 0.1	13.3 ± 0.4	22.18 ± 0.07
Total	96.3	96.04	98.5

Table 2
Average concentration of trace element by pressed pellet (XRF) reported as mean ± the confidence interval (t-distribution) of 3 replicates.

mg kg^{-1}	Medium MSW IBA	Fine MSW IBA	<1.18 mm fraction
S	6070 ± 130	10,900 ± 300	16,400 ± 300
Cl	4290 ± 60	8890 ± 350	17,100 ± 50
Zn	5250 ± 200	6970 ± 40	7600 ± 110
Cu	1420 ± 80	3220 ± 80	3550 ± 60
Ba	1970 ± 700	1380 ± 230	1350 ± 620
Sr	1430 ± 20	442 ± 7	464 ± 14
Cr	618 ± 70	853 ± 52	863 ± 97
Pb	416 ± 40	774 ± 78	1100 ± 60
Sn	171 ± 20	296 ± 19	412 ± 40
Zr	338 ± 440	198 ± 51	127 ± 13
Ni	93.0 ± 20	159 ± 12	218 ± 7
Mo	N/D (<1)	N/D (<1)	275 ± 448
Cd	N/D	N/D	N/D

3.1.5. Microscopic description and elemental composition of MSW IBA components

SEM observation showed the MSW IBA is dominated by phases whose morphology and EDX spectra suggests are primary and secondary glass (Fig. 1). These phases are prevalent in larger particles (as indicated by the macroscopic classification and XRD analysis) as well as widely present as a constituent of fine particles and aggregations. Primary glass has a distinct sodic composition (SI Table S.4) and smooth texture.

Secondary glass on the other hand has a more variable composition, with Ca-rich variants, as well as Al, K and Fe rich variants (SI Table S.4), and textures associated to the melting process such as abundant vesicles (empty or filled with fine ash), flow structures delineated by glass of different compositions, exsolution of wollastonite crystals, and abundant inclusions of fine particles. A gradation between primary and secondary glass is often observed in particles with a nucleus of primary glass that grades to secondary glass towards the edges.

Fine particles are present as loose individual particles, in aggregations, as a layer covering larger particles and as inclusions in secondary glass. Quartz grains are a major constituent of this fraction, but it also contains secondary glass, Al-rich phases, Fe-oxides and Ca associated to S and P. The remaining fine particles have varying compositions, but some contain Ti, Mg and Ba. When fine particles are present in aggregations or as layers on other particles, the cementing matrix is dominated by Ca, followed by Al (Fig. 1).

PTEs (Zn and Cu) are detected in the EDX spectra only at very low concentration close to the detection limit (≤0.1 At%) and in maps do not appear to be associated to specific phases, but rather are dispersed in both the fine particles and secondary glass. With point analysis, however, Fe rich particles are the only ones to show some Cu and Zn (though in equally low concentrations) (see SI Table S.4).

3.1.6. Speciation of Zn and Cu in MSW IBA

Bulk XANES spectra for the two most abundant PTEs, Zn and Cu, were collected from multiple points in each sample (Medium MSW IBA, Fine MSW IBA and < 1.18 mm fraction). Fig. 2 shows the merged (averaged) spectra for each sample, along with spectra from standards. For both metals the spectra were similar for all three samples analysed, indicating the speciation of these elements is similar in the different sized IBA fractions.

The bonding environments that best matched the IBA Zn-XANES spectra were oxygen-bound and (HFO)-adsorbed Zn (Zn(II)-O and Zn (II)-ads) (see Fig. 2). The optimum linear combination fit (LCF) was given by ~ 40 % Zn(II)-O, ~40 % Zn(II)-ads, ~20 % Zn(II)-S phases. A small percentage (~10 %) of Zn(II)–CO_3 in the LCF was also possible, however this did not greatly improve the "goodness of fit". There is no evidence in the Zn-XANES spectra for the presence of metallic Zn or Zn

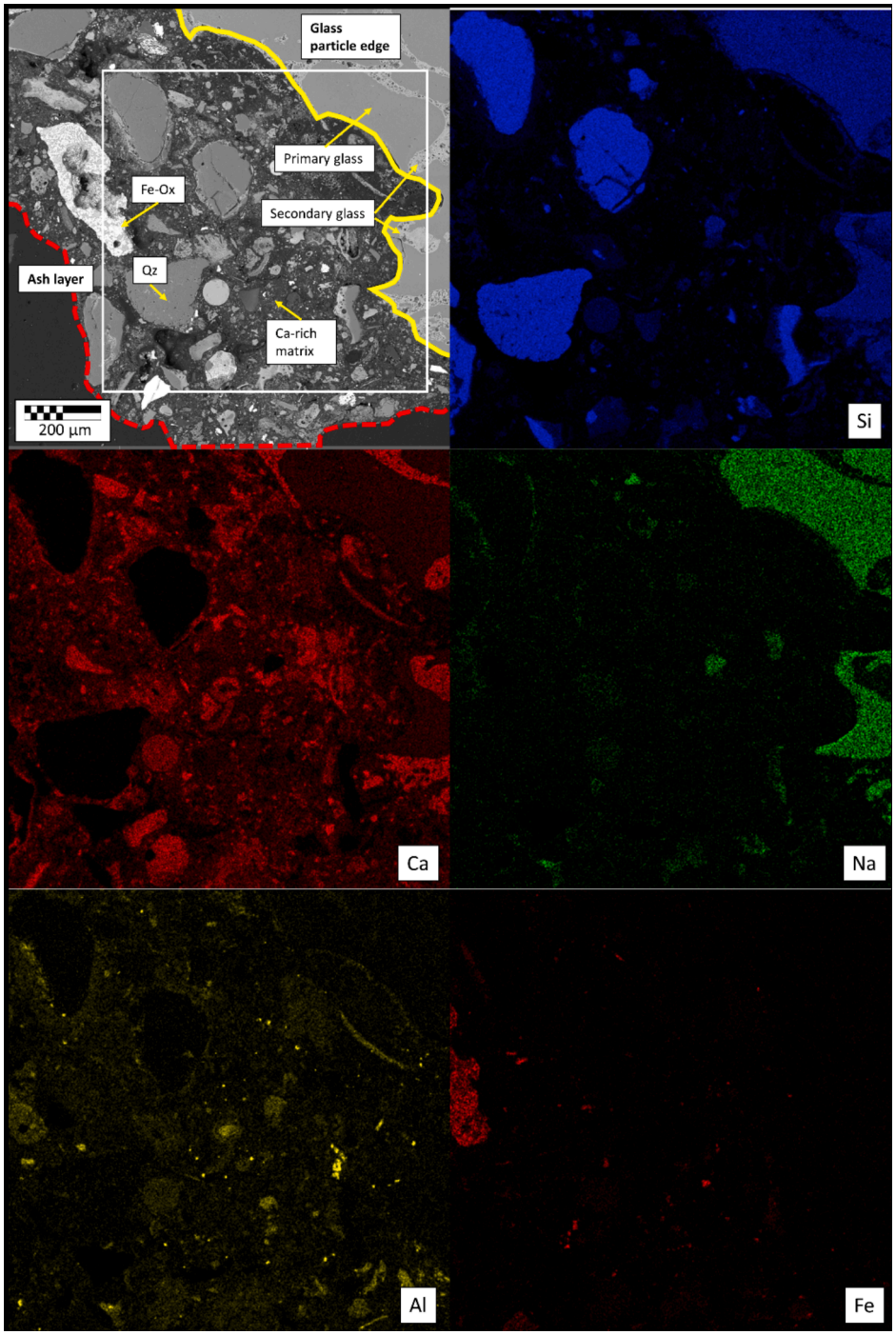

Fig. 1. SEM backscatter image of MSW IBA showing characteristic components and their composition in EDX elemental maps. The square outline in white in the first panel indicates area covered by the elemental mapping.

alloys such as brass in the MSW IBA samples.

The bonding environments that best matched the IBA Cu-XANES spectra was Cu(II)-O. This could be LCF modelled by using either the spectrum for hydrous ferric oxide (HFO)-adsorbed (ads) Cu(II) alone (as shown in Fig. 2), or a mixture of the Cu(II)-ads and Cu(II)–CO_3 spectra. As both produced similar "goodness of fit", the simpler option (Cu(II)-ads alone) was used. The optimum LCF was given 45–50 % Cu(II)-ads, 20–30 % Cu(I)-S, and (25–35 %) Cu(I)-O. There is no evidence in the Cu-XANES spectra for the presence of metallic Cu in the MSW IBA samples.

3.1.7. *Persistent organic pollutants (POPs)*

Persistent organic pollutants (POPs) were measured in the fine MSW IBA. All PAHs were undetectable. PCDDs/PCDFs and PCBs were detected at low concentrations (average PCDDs/PCDFs and PCBs concentrations were 1.78 TEQ ng kg^{-1} and 0.008 TEQ ng kg^{-1} using the WHO 2005 TEQ calculation for humans; SI Table S.5).

3.2. *pH dependant batch leaching*

The fine MSW IBA is a highly alkaline material that equilibrated with deionised water at a pH of ~ 11.3 (Fig. 3). Approximately 1.5 mol of acid (H+) per kg of ash was required to produce a pH of 7. The solution

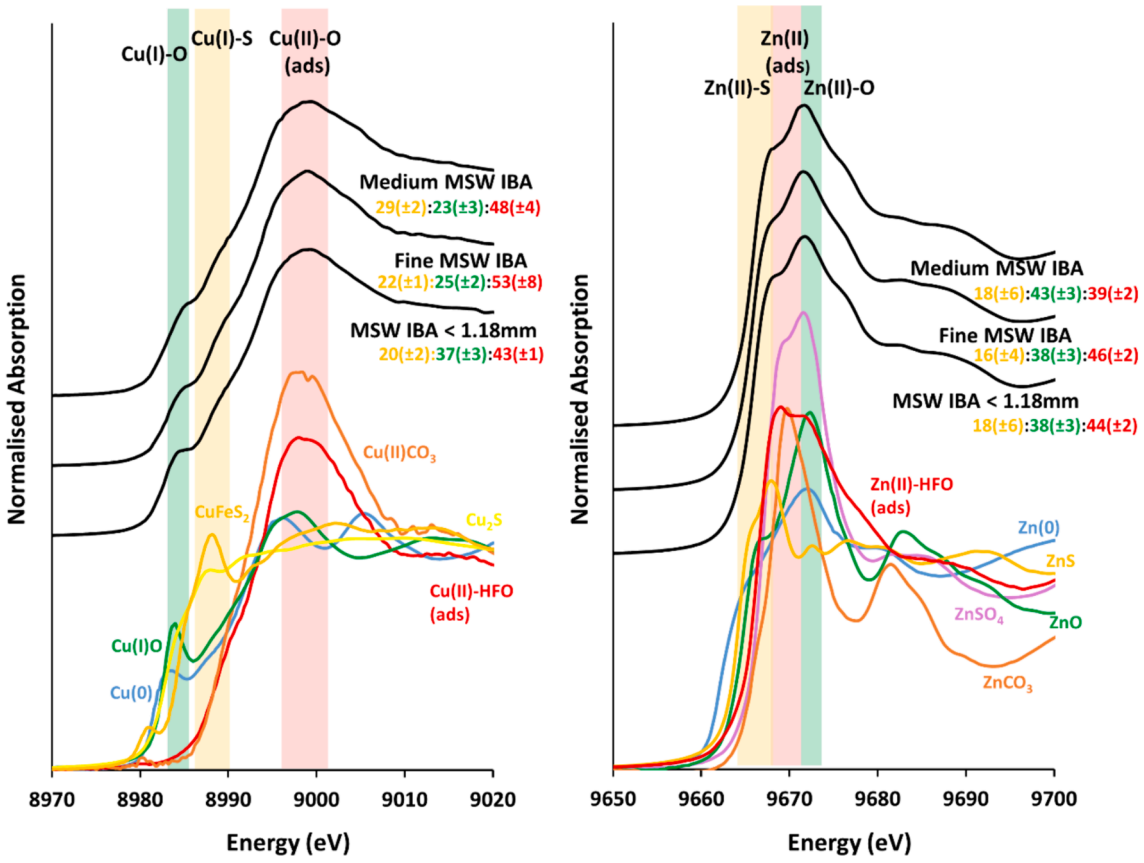

Fig. 2. Bulk average K-edge XANES spectra for Cu and Zn collected from MSW ash samples and selected standards. Ratios presented below the sample names are results for LCF analysis of the sample spectra (Cu, Zn), colours used match to the standards shown. The coloured bands are provided to guide the eye to significant spectral features present in standard spectra.

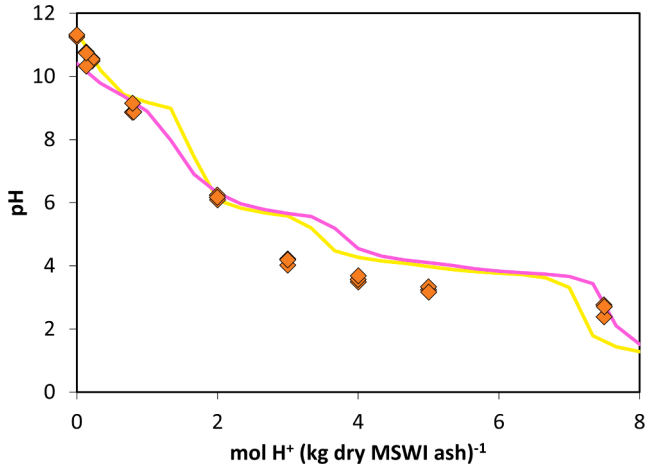

Fig. 3. Acid neutralization curve of the fine MSW IBA. Yellow and pink lines correspond to PHREEQc models for dissolution and dissolution + surface sorption respectively. (For interpretation of the references to colour in this figure legend, the reader is referred to the web version of this article.)

composition at pH 11.3 is dominated by Na^+ and K^+, but when the solution pH was brought below pH 10 by acid addition Ca^{2+} became the dominant ion in solution (Fig. 5) throughout the rest of the pH range. Sulphur was released to solution as the pH decreased below 11.3, and Mg was released to solution when the pH<9. Very little Fe, P and Si were released to solution until the pH was ≤ 4. Al appears in solution in low concentrations at pH>10, and then again at pH ≤ ~4 at higher concentrations.

The pH dependant batch leaching tests indicated that most PTEs contained in MSW IBA are not released until the solution pH decreases below pH 4 (although low concentrations of Cd begin to be released when the pH is below 7, Ni and Zn are released to solution at pH~6, with increasing concentrations in solutions with lower pH; Fig. 4). Cu, Cr, Pb, Sn contained in the IBA are not released to solution in appreciable quantities until the pH<4. Interestingly, while the concentrations are low, Mo shows amphoteric behaviour with leaching occurring at both high (>6) and low (<2) pH values.

3.3. Environmental lixiviants and metal leaching

When increasing amounts of wood chips (0, 1, 2, 3, 4, 5 g) were added to leaching tests containing 15-20 g of MSW and 200 mL of deionised water, there was a linear increase in DOC (from 0.7 to 4.8 mg DOC per g of MSW IBA; Fig. 6). There was an accompanying reduction in solution pH, from 11.3 with deionised water, to 9.9 with 25 % wood chips. The most dilute synthetic exudate solution, which is representative of real systems, had only a very small effect on the solution pH. This solution produced a solution at pH 11.2 with 0.9 mg DOC per g of MSW IBA. Increasing exudate concentration reduced the pH of the solution, and increased the DOC concentration, with the highest exudate concentration equilibrating at pH 7.8 with 130 mg DOC per g MSW IBA.

Overall, the leaching behaviour of MSW IBA in solutions containing wood chips was similar to that with HNO_3 (Figs. 4 and 5). At the same pH value, the Na and K concentrations were slightly higher in tests containing wood chips, than in tests where the pH was adjusted with HNO_3 (particularly with larger wood chip additions). Similarly, the concentrations of the trace metals Cr and Mo, were slightly higher where

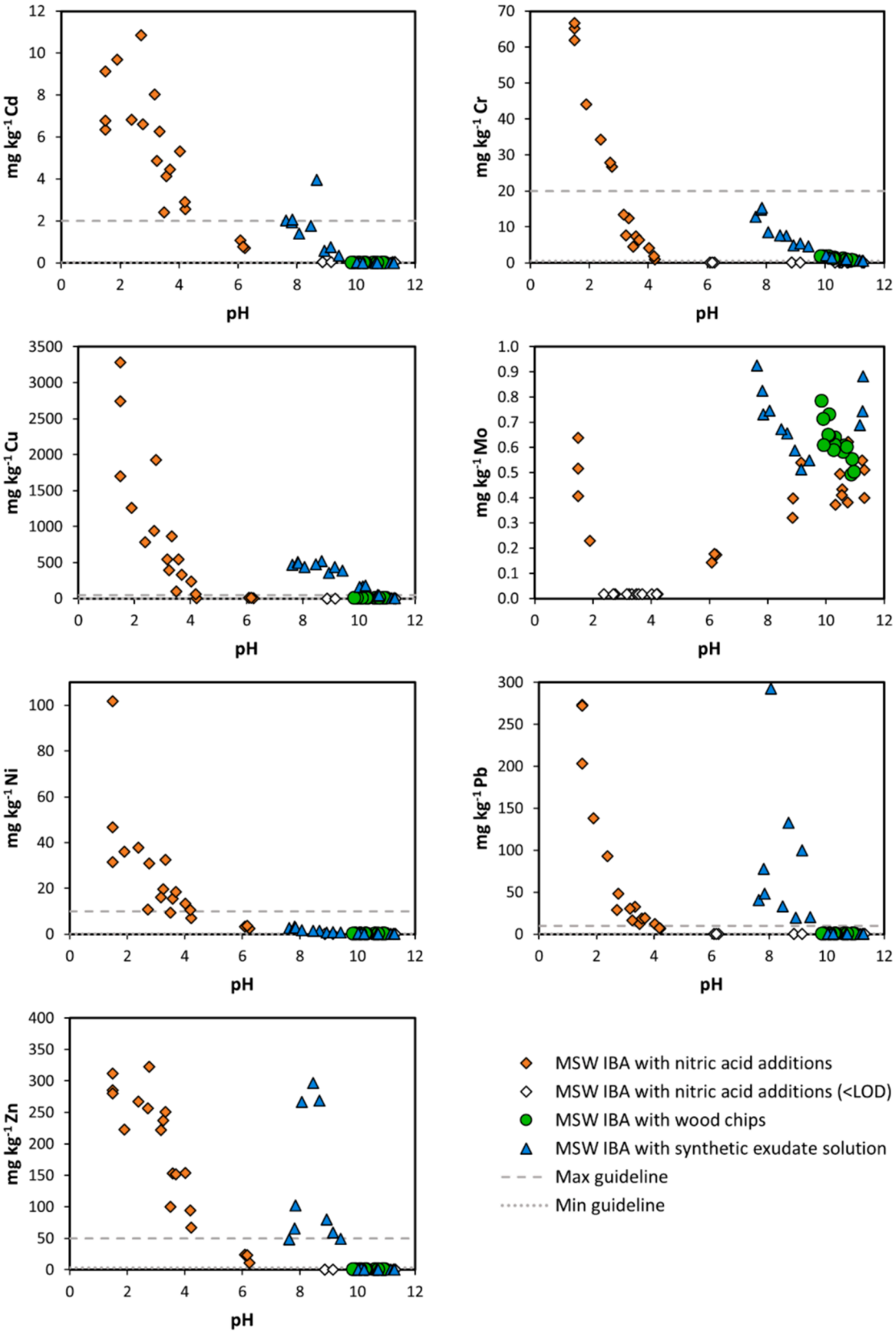

Fig. 4. leaching behaviour of PTEs's (expressed in mg PTE per kg of MSW IBA) vs solution pH. European guideline values (Table S.7) obtained from Blasenbauer et al (2020) and reference therein (Government-of-Wallonia, 2001 (last modified in 2018), Blasenbauer et al., 2020; Swedish-EPA, 2010; RIVM, 2007; Lithuanian-Government, 2016; Valorsul, 2017; Flemish-Government, 2012; Republic-of-Austria, 2017a; Republic-of-Austria, 2017b; Italian-Republic, 2006; Italian-Republic, 1998; French-Republic, 2011; LAGA, 1995a; LAGA, 1995b)).

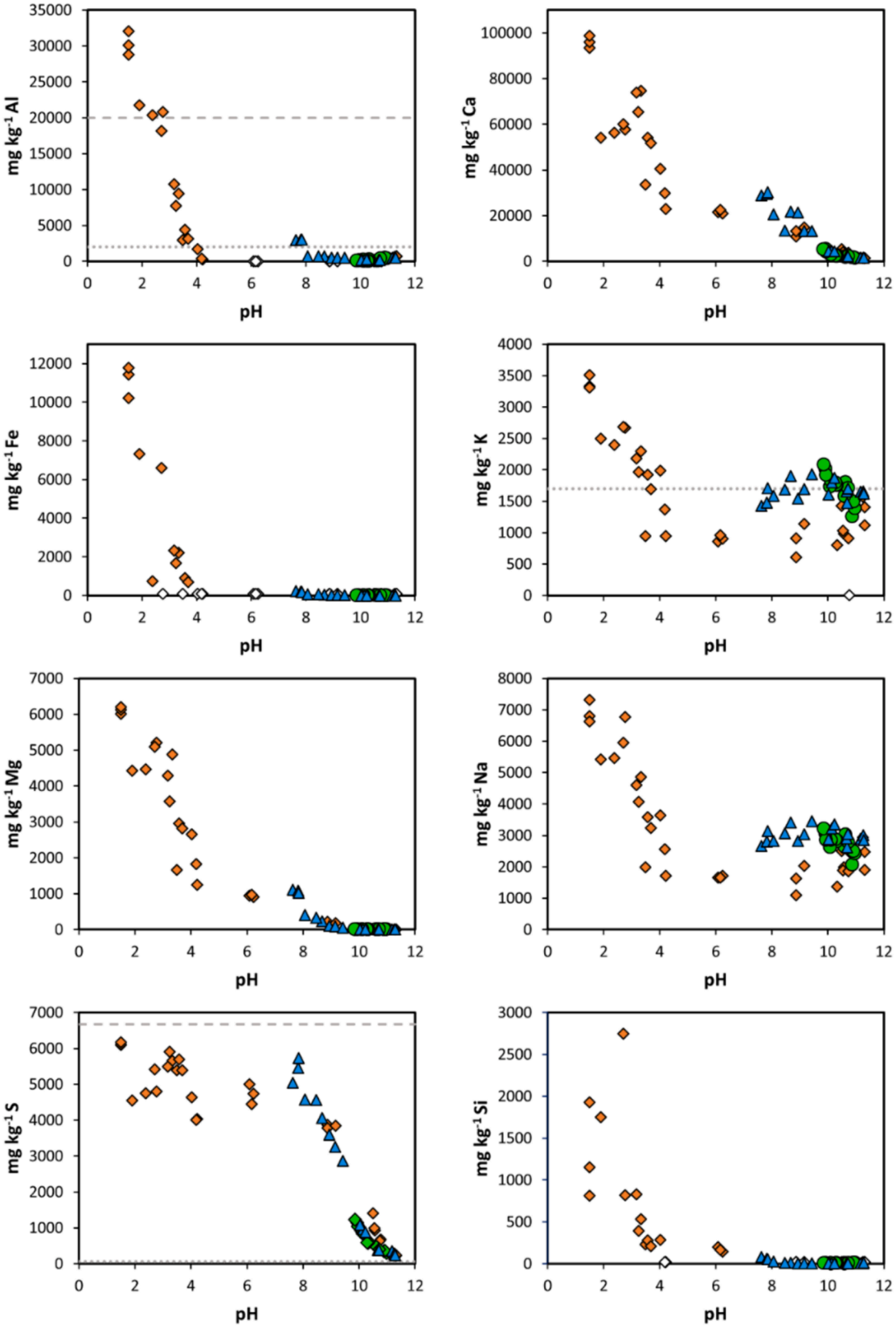

Fig. 5. leaching behaviour of selected major elements (expressed in mg of a major element per kg of MSW IBA) vs solution pH. Same legend description as that of Fig. 4. European guideline values (Table S.7) obtained from Blasenbauer et al (2020) and reference therein (Government-of-Wallonia, 2001 (last modified in 2018), Blasenbauer et al., 2020; Swedish-EPA, 2010; RIVM, 2007; Lithuanian-Government, 2016; Valorsul, 2017; Flemish-Government, 2012; Republic-of-Austria, 2017a; Republic-of-Austria, 2017b, Italian-Republic, 2006; Italian-Republic, 1998; French-Republic, 2011; LAGA, 1995a; LAGA, 1995b)).

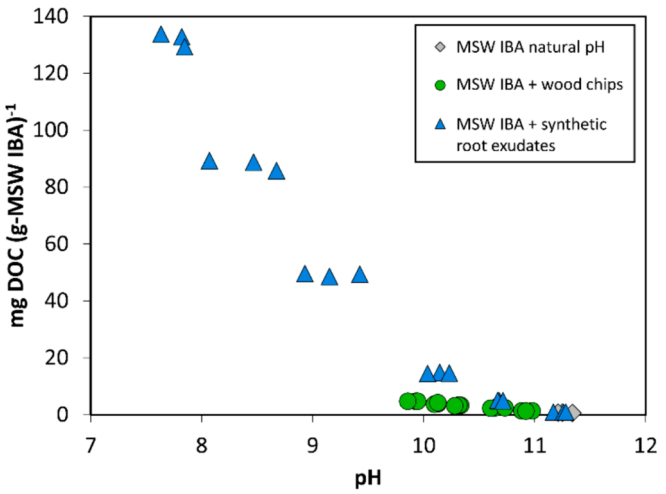

Fig. 6. mg of DOC in the supernatant per g of MSW IBA vs solution pH in batch leaching tests with environmental lixiviants.

the tests contained wood chips. However, the differences to the MSW IBA with nitric acid additions were small.

The leaching behaviour of both major and trace elements with the synthetic exudate solution was similar to that of MSW IBA with HNO_3 when exudate concentration was $\leq$ 1,500 mg l^{-1} DOC (a range which corresponds with pH>10). When synthetic exudate addition was sufficient to buffer the pH<10, the PTEs Cd, Cr, Cu, Mo, Pb, Zn, as well as the major elements K and Na had higher concentrations in the leachate than those in MSW IBA with HNO_3 at a similar pH. At the highest synthetic exudate concentration (~13,000 mg l^{-1} DOC and leachate pH<8), the concentrations of Al, Ca and S are slightly higher than in tests where the pH was adjusted with HNO_3.

4. Discussion

4.1. MSW IBA composition

Silica was identified as the major component of the MSW IBA samples, present in primary and secondary glass and quartz particles. The decrease in SiO_2 concentration in samples with smaller particle sizes is also consistent with the observed predominance of glass amongst larger particles (similarly Na, the 5th most abundant element in MSW IBA, and an important constituent of commercial glass (Ashby, 2013; Mirsayar et al., 2017), exhibited a decrease in concentration with particle size). The finding that primary and secondary glass are the most abundant components of MSW IBA agrees with previous work (Blasenbauer et al., 2020; Wei et al., 2011; CEWEP, 2016; Chandler et al., 1997; Chimenos et al., 1999; Holm and Simon, 2017; Huber et al., 2020; Aubert et al., 2006; Zhu et al., 2020; Loginova et al., 2019). Recently, primary and secondary glass represented about 60 wt% in MSW IBA from Spain, despite a reduction over the recent decades (del Valle-Zermeño et al., 2017). The entrapment of other phases (quartz, ash clusters and metals) within secondary glass (a melt phase) may, however, be leading to some overestimation of its mass proportionally to these other phases.

The second most abundant element in all samples was Ca, increasing in MSW IBA samples with predominance of smaller particle sizes. SEM-EDX elemental mapping showed that Ca was a major element in aggregations and surface layers and XRD identified calcite and ettringite as the third and fourth most abundant minerals. Accumulation of Ca in fine ash and the presence of ettringite in quenched and/ or weathered MSW IBA has also been reported by others (Alam et al., 2019; Zhu et al., 2020; Loginova et al., 2019; Meima and Comans, 1997). Sources of Ca in MSW include industrial materials (e.g. construction waste), soil particles (Alam et al., 2019) and finely ground Ca-rich materials (such as limestone, chalk and gypsum) widely used as fillers in the manufacture of paper and plastic packaging (second and third most abundant waste types in UK MSW after kitchen and garden waste (Burnley, 2007)).

Fe and Al are the third/ forth most abundant elements determined by XRF analysis and were consistently present in the EDX elemental maps. Both are seen in high Fe or Al particles (free or as inclusions in secondary glass) and as a constituent of secondary glass. The concentration of Al increased with decreasing ash particle sizes, and it is an important constituent of the matrix of aggregations and in ash layers covering other particles. Like Ca, the main sources of Al in MSW IBA are probably fillers used in paper and plastic packaging (Murray, 2006; Bonadies et al., 2022). The concentration of Fe did not show any trend with the PSD of samples. Ferrous metals form about 4 % of UK MSW (Burnley, 2007), and while larger metal particles are magnetically recovered during ash processing, smaller particles and rust flakes will remain in the IBA.

Zn and Cu concentrations in bulk samples (determined by XRF) increased in MSW IBA samples with smaller particle sizes (like other heavy metals) indicating that these metals were preferentially associated with finer particles. In SEM-EDX elemental maps, Zn and Cu were mostly evenly distributed in the fine matrix rather than associated with specific phases, however, some high Fe- particles had Cu and Zn in their composition.

XANES analysis suggests that Zn was predominantly present in the MSW IBA as absorbed Zn(II) in inner sphere complexes associated with metallic oxides (e.g. Zn(II)-HFO), as well as Zn(II) oxides (e.g. ZnO) and sulphides (e.g. sphalerite, ZnS). Similarly, for Cu, the best fit was given by a combination Cu(II) in inner sphere complexes associated with metallic oxides (e.g. Cu(II)-HFO), as well as Cu(I) oxides (e,g. Cu_2O) and sulphides (e.g. covalite, CuS). Previous work based on SEM-EDX analysis and electron microprobe analysis has suggested that Cu in MSW IBA is found as Cu-sulfides, and both Zn and Cu are found as spinels and metallic particles, often present as inclusions in secondary glass (Wei et al., 2011; Šyc et al., 2020; Bayuseno and Schmahl, 2010). However, the XANES data are not consistent with either a significant proportion of metallic Cu or Zn, or with Cu in spinels in this MSW IBA. It suggests that larger metallic particles (e.g. remnants of copper wire, brass, Zn-C batteries) are successfully removed from the MSW IBA at this plant, and that any small metallic Cu and Zn particles are oxidized during incineration and quenching (Šyc et al., 2020; Cheng et al., 2023). Also, while the quenching and/or weathering of MSW IBA leads to the formation of hydrate secondary minerals (e.g., ettringite, hydrocalumite and calcium-silicate-hydrate phases) into which divalent metals can substitute for Ca^{2+}, the XANES data are not consistent with a significant proportion of Cu or Zn present in such weathering products.

The POPs of most concern in incineration ashes, where they are unintentionally produced as a byproduct of combustion, are PAHs, PCDD/Fs and PCBs (Freire et al., 2015; Swedish-EPA, 2011; UNEP, 2001). These POPs, which condense onto the ash from the flue gases, tend to have higher concentrations on fine particles due to their higher specific surface area. However, no PAHs were detectable in the fine MSW IBA. Similarly, PCDDs/PCDFs and PCBs concentrations in the fine ash were substantially lower than reference regulatory limits in all replicates tested (SI Table S.5). Combustion temperature, furnace technology (particularly the bottom ash cooling regime), and ash size fraction are thought to be the major determinants of the POPs concentrations in combustion ashes (Chagger et al., 1998; Khan et al., 2009; Peng et al., 2016). This work suggests that even fine MSW IBA can meet regulatory limits for POPs, if a suitable combustion temperature is maintained in a modern incineration facility.

4.2. Leaching behaviour of MSW IBA

The major components of the MSW IBA, glass and ceramics, leach very slowly at high pH values (Abraitis et al., 2000), therefore the solution composition of water in contact with the IBA is primarily

controlled by the pH dependant leaching of the reactive minor phases present. When the solution pH was calculated in PHREEQC (as a function of H^+ addition and dissolution of the suite minerals based on the XRD analysis; SI Table S.3) the resultant dissolution model (Fig. 3) approximated the acid neutralisation data. Therefore, it should be possible to predict IBA pH buffering behaviour using the crystalline phases present. However, with the pH stability of these minerals alone, some segments of pH buffering remain unexplained, and could be attributed to poorly crystalline phases not captured by XRD or reaction occurring in the leachate, including precipitation of newly formed phases at certain pHs.

When MSW IBA is equilibrated with deionised water, the leachate is buffered to ~ pH 11.3 primarily by dissolution of Na, Ca and K containing phases (probably phases such as NaOH, $Ca(OH)_2$ and KOH that formed during MSW incineration (Meima and Comans, 1997; Belevi et al., 1992)). About 8 % and 17 % of the total Na and K, but only 1 % of total Ca were released with deionised water. Only a proportion of Na and K were leached at any pH value (~25 % and 40 %), probably because they were associated with the glass phases, but most Ca in the MSW IBA is leachable (~85 %), so most must be in Ca-rich phases that are not readily hydrated by water to produce alkalinity.

When the addition of acid reduced the pH below 11 the concentration of both Ca and S increased, suggesting dissolution of the ettringite (hydrous calcium aluminium sulphate) present in the IBA. Ettringite is highly insoluble above pH 10.7, but dissolves incongruently between 11 > pH>9 to produce Ca^{2+}, SO_4^{2+} (which may result in formation of gypsum) and insoluble aluminium (oxy)hydroxides, possibly along with calcium aluminates like hydrocalumite, given the availability of Ca (Langmuir, 1997; Myneni et al., 1998; Meima and Comans, 1997; Mantovani et al., 2023). This explains why Al is present in the leachate at pH>10, but becomes undetectable bellow that pH, until it reappears at pH≤4. Below pH 9, carbonates (including calcite) present in the MSW IBA will dissolve, and Ca was indeed the principal element released to solution between 9 > pH>6, (along with some Mg, which may have been present as an impurity in carbonates). Between pH 6 and 4 concentration of the major ions remain relatively constant suggesting that no additional phases are leached until the pH of the leachate was below pH 4. In this range the carbonate equilibrium (the acid-base system between carbonic acid [H_2CO_3] and bicarbonate [$HCO_3 + H^+$], equilibrium at pH ≈ 5 (Lockwood et al., 2014)) can contribute to buffer the pH in the system. At low pH (pH<4), the solution concentrations of Ca, Al, Fe, Si, Mg, Na and K increase with decreasing pH value, with Ca and Al dominating the leachate composition (Figure S.7). This is compatible with dissolution of $Al(OH)_3$ (Figure S.8) alongside calcium aluminates, iron oxide and feldspars (hematite, magnetite, microcline and albite were all observed by XRD) (Jang et al., 2007; Vehmaanperä, 2022; Yuan et al., 2019; Casey et al., 1991). In addition, below pH 4 the rate of silicate glass dissolution also increased (Abraitis et al., 2000), which may have added more Na, Si, Al and Fe to solution.

Essentially all the PTE elements measured (Cr, Pb, Zn, Cu, Ni, Mo, Cd) have broadly similar leaching behaviours at low pH values. Leaching below pH 4 coincides with the bulk dissolution of the major phases present and high concentrations of H^+ as competing ions for surface absorption sites (e.g. $Al(OH)_3$). Cu and Zn were found in a mix of absorbed, oxide and sulphide phases, which would also potentially be leached at low pH (Millward and Moore, 1982; Beverskog and Puigdomenech, 1997; Wang et al., 2022; Young et al., 2003); similar associations are likely to account for the increased leaching of other PTEs at low pH. Despite being present in a similar types of phases, Cu is much less resistant to leaching in acids compared to Zn (and the other metals present) and is therefore likely to be more easily recovered from MSW IBA. Cd (and to a lesser extent Ni and Zn) was moderately leached at around pH 6, this may be explained by association with carbonates which are dissolved at this pH (Sjöberg and Rickard, 1984). Mo was the only PTE present that was significantly leached at high pH. In oxidising environments at high pH Mo(VI) is predicted to be present as the molybdate oxyanion which is soluble in high pH solution and weakly sorbs to any surfaces present (Weidner and Ciesielczyk, 2019).

It required addition of approximately 1.5 and 3 mol H^+ per kg of MSW IBA to buffer the leachate pH value to 7 and 4, respectively (n.b. 1.5 mols H^+ is equivalent to leaching by 150,000 L of rainwater (@pH5) per kg of IBA). Therefore, reaching pH 4, the threshold below which the release of contaminant metals becomes problematic, is unlikely by natural infiltration or carbonation.

MSW IBA was leached with two solutions that are representative of the environmental lixiviants that could be found close to a structure, such as a road, where MSW IBA may be reused (plant exudates may be released from a vegetated soil layer, and a solution similar to wood chip leachate from forest litter). Leaching with woodchips as a source of DOC results in only a modest reduction in solution pH compared to leaching in deionised water alone, even though the ratio of wood chips to MSW IBA was representative of an extreme situation such as a stockpile of wood chips on top of a layer of IBA. Even so, the resultant PTE concentrations in solution did not greatly deviate from those in the nitric acid leaching experiments at the same pH value. Thus, mobilisation of contaminant metals by infiltration with water containing DOC due to contact with forest litter (a composition dominated by lignins, tannins and phenolic compounds (Kannepalli et al., 2016; Taylor and Carmichael, 2003; Tao et al., 2005)) is very unlikely to become problematic.

To represent the long-term effects of leaching with plant exudates, the synthetic exudate solutions were up to two orders of magnitude more concentrated than the solutions produced by vegetative cover. These solutions resulted in pH values between 7–10, and aqueous Cd, Cu, Cr, Pb and Zn concentrations that were only exceeded in the nitric acid leaching tests when the pH value was below pH 4. Cu, which had the highest concentration in the exudates leachate, is known to have affinity with organic complexes, and has been detected in MSW IBA leachate almost entirely complexed with hydrophilic DOC and/ or fulvic acid derived from the ash (Olsson et al., 2007; Meima et al., 1999; Arickx et al., 2010; Johnson et al., 1999). In tests carried out here, the input of well-known organic ligands, such as citrate, via the synthetic root exudate solutions, may have had the effect of stabilising metals in solution by competing with surface sorption sites (e.g. Al and Fe ox/hydroxides) (Weng et al., 2002; Inskeep and Baham, 1983; Violante, 2013; Caporale and Violante, 2016; Agnello et al., 2014; Meima et al., 1999; Yan et al., 2022), and thus the leaching data supports the notion that a portion of the metals are present in sorption complexes on mineral surfaces rather than incorporated into crystalline phases.

However, it is important to note that the concentrations of exudates produced by vegetative cover is generally low (<100 mg DOC l^{-1} (Strohmeier et al., 2013; Worrall et al., 2004; Clay et al., 2009; Adeleke et al., 2017)), which is comparable to the most dilute synthetic exudate solution used (50 mg DOC per L). Also, in natural systems, the majority of plant exudates are consumed in the rhizosphere by microorganisms (bacteria and fungi) and by plant roots (Adeleke et al., 2017; Kuzyakov et al., 2003; van Hees et al., 2005; Fischer et al., 2007). However, if an undiluted exudate solution from a vegetative cover layer were to permeate MSW IBA continually over a long period, it has the potential to facilitate the buffering of pH downwards and form complexes with a small proportion of sorbed metals. In this unlikely situation, a small release of contaminant metals would occur with each pore volume of flow, but the resulting aqueous concentration would be extremely low (likely much less than guideline values for groundwater shown in Fig. 4). Outside of naturally occurring DOC, there could, however, be potential in the use of artificially concentrated organic lixiviants as a pretreatment for MSW IBA, to reduce the content of heavy metals available for leaching, prior to re-use.

5. Conclusions

MSW IBA produced from waste from a major UK city contained PTEs at total concentrations that exceed most guidelines for unrestricted

environmental use. However, only a small proportion of these PTEs can be mobilised to aqueous solution unless the pH is reduced to well below pH5 (a typical value for rainwater). In common with most other MSW IBAs, this material has a very high acid buffering capacity, and it would take approximately a million pore volume replacements by typical UK rainfall to reach pH 5. Thus, mobilisation of problematic concentrations of PTEs from this IBA by rainwater is extremely unlikely, and use of this MSW IBA for specified construction activities does not pose an environmental hazard.

If plant exudates from surface vegetation are allowed to directly permeate MSW IBA over a long period, they will slightly increase the rate at which the pH is buffered downwards, and slightly increase the mobility of some contaminant metals at moderately alkaline pH values (e.g. Cu and Mo). However, the concentrations of any contaminant metals mobilised by a representative exudate solution are very low and, in natural systems, the majority of plant exudates are consumed in the rhizosphere, and thus the risk posed by plant exudates is low.

In MSW IBA from a modern, tightly regulated, energy-from-waste plant, PAHs were undetectable, and PCDDs/PCDFs and PCBs concentrations well below reference regulatory limits. Thus, POPs are not an environmental concern for this IBA.

CRediT authorship contribution statement

Felipe E. Sepúlveda Olea: Writing – original draft, Visualization, Methodology, Validation, Formal analysis, Investigation, Conceptualization. **Ian T. Burke:** Writing – review & editing, Supervision, Methodology, Investigation, Funding acquisition, Conceptualization. **Arif Mohammad:** Methodology, Formal analysis. **Douglas I. Stewart:** Writing – review & editing, Supervision, Methodology, Investigation, Funding acquisition, Conceptualization, Project administration.

Declaration of competing interest

The authors declare that they have no known competing financial interests or personal relationships that could have appeared to influence the work reported in this paper.

Data availability

Data will be made available on request.

Acknowledgements

We thank SUEZ Recycling and Recovery UK Ltd for providing the MSW IBA used in this study. We acknowledge support from Engineering and Physical Science Research Council grant EP/T031166/1 and EP/T03100X/1, Diamond Light Source for time on Beamline I18 under Proposal SP33049 and help from beamline scientist, Stuart Bartlett. Lesley Neve, Stephen Reid, Jianting Feng, Richard Walshaw and John Wyn Williams are also acknowledged for help during XRD, XRF, ICP-OES/MS, XAS and SEM/EDX analysis.

Appendix A. Supplementary data

Detailed description of methodologies and additional figures and data tables are included in the Supplementary data to this article can be found online at https://doi.org/10.1016/j.wasman.2024.07.026.

References

Abraitis, P.K., Livens, F.R., Monteith, J.E., Small, J.S., Trivedi, D.P., Vaughan, D.J., Wogelius, R.A., 2000. The kinetics and mechanisms of simulated British Magnox waste glass dissolution as a function of pH, silicic acid activity and time in low temperature aqueous systems. Appl. Geochem. 15, 1399–1416.

Adeleke, R., Nwangburuka, C., Oboirien, B., 2017. Origins, roles and fate of organic acids in soils: a review. S. Afr. J. Bot. 108, 393–406.

Agnello, A.C., Huguenot, D., Van Hullebusch, E.D., Esposito, G., 2014. Enhanced phytoremediation: a review of low molecular weight organic acids and surfactants used as amendments. Crit. Rev. Environ. Sci. Technol. 44, 2531–2576.

Alam, Q., Schollbach, K., van Hoek, C., van der Laan, S., de Wolf, T., Brouwers, H.J.H., 2019. In-depth mineralogical quantification of MSWI bottom ash phases and their association with potentially toxic elements. Waste Manage. 87, 1–12.

Arickx, S., De Borger, V., Van Gerven, T., Vandecasteele, C., 2010. Effect of carbonation on the leaching of organic carbon and of copper from MSWI bottom ash. Waste Manage. 30, 1296–1302.

Ashby, M. F. 2013. Chapter 15 - Material profiles. *In:* ASHBY, M. F. (ed.) *Materials and the Environment (Second Edition)*. Boston: Butterworth-Heinemann.

Aubert, J.E., Husson, B., Sarramone, N., 2006. Utilization of municipal solid waste incineration (MSWI) fly ash in blended cement: Part 1: processing and characterization of MSWI fly ash. J. Hazard. Mater. 136, 624–631.

Bayuseno, A.P., Schmahl, W.W., 2010. Understanding the chemical and mineralogical properties of the inorganic portion of MSWI bottom ash. Waste Manage. 30, 1509–1520.

Belevi, H., Stämpfli, D.M., Baccini, P., 1992. Chemical behaviour of municipal solid waste incinerator bottom ash in monofills. Waste Manage. Res. 10, 153–167.

Beverskog, B., Puigdomenech, I., 1997. Revised pourbaix diagrams for copper at 25 to 300°C. J. Electrochem. Soc. 144, 3476–3483.

Blasenbauer, D., Huber, F., Lederer, J., Quina, M.J., Blanc-Biscarat, D., Bogush, A., Bontempi, E., Blondeau, J., Chimenos, J.M., Dahlbo, H., Fagerqvist, J., Giro-Paloma, J., Hjelmar, O., Hyks, J., Keaney, J., Lupsea-Toader, M., O'Caollai, C.J., Orupõld, K., Pajak, T., Simon, F.-G., Svecova, L., Šyc, M., Ulvang, R., Vaajasaari, K., Van Caneghem, J., van Zomeren, A., Vasarevičius, S., Wégner, K., Fellner, J., 2020. Legal situation and current practice of waste incineration bottom ash utilisation in Europe. Waste Manage. 102, 868–883.

Bonadies, I., Capuano, R., Avolio, R., Castaldo, R., Cocca, M., Gentile, G. & Errico, M. E. 2022. Sustainable Cellulose-Aluminum-Plastic Composites from Beverage Cartons Scraps and Recycled Polyethylene. *Polymers* [Online], 14.

Brunner, P.H., Rechberger, H., 2015. Waste to energy – key element for sustainable waste management. Waste Manage. 37, 3–12.

BSI, 2022. Methods of Test for Soils for Civil Engineering Purposes – Classification Tests and Determination of Geotechnical Properties. BSI, UK.

Burnley, S.J., 2007. A review of municipal solid waste composition in the United Kingdom. Waste Manage. 27, 1274–1285.

Caporale, A.G., Violante, A., 2016. Chemical processes affecting the mobility of heavy metals and metalloids in soil environments. Current Pollution Reports 2, 15–27.

Casey, W.H., Westrich, H.R., Holdren, G.R., 1991. Dissolution rates of plagioclase at pH = 2 and 3. Am. Mineral. 76, 211–217.

Cewep, 2016. Bottom Ash Factsheet. Belgium, Brussels.

Chagger, H.K., Kendall, A., McDonald, A., Pourkashanian, M., Williams, A., 1998. Formation of dioxins and other semi-volatile organic compounds in biomass combustion. Appl. Energy 60, 101–114.

Chandler, A. J., Eighmy, T. T., Hartlén, J., Hjelmar, O., Kosson, D. S., Sawell, S. E., van der Sloot, H. A. & Vehlow, J. 1997. Chapter 9 - Bottom ash. *Municipal Solid Waste Incinerator Residues*. Elsevier, 339-418.

Chen, D.-M.-C., Bodirsky, B.L., Krueger, T., Mishra, A., Popp, A., 2020. The world's growing municipal solid waste: trends and impacts. Environ. Res. Lett. 15, 074021.

Cheng, S., Ding, X., Dong, X., Zhang, M., Tian, X., Liu, Y., Huang, Y., Jin, B., 2023. Immigration, transformation, and emission control of sulfur and nitrogen during gasification of MSW: fundamental and engineering review. Carbon Resour. Convers. 6, 184–204.

Chimenos, J.M., Segarra, M., Fernández, M.A., Espiell, F., 1999. Characterization of the bottom ash in municipal solid waste incinerator. J. Hazard. Mater. 64, 211–222.

Clay, G.D., Worrall, F., Fraser, E.D.G., 2009. Effects of managed burning upon dissolved organic carbon (DOC) in soil water and runoff water following a managed burn of a UK blanket bog. J. Hydrol. 367, 41–51.

Crillesen, K., Skaarup, J., 2006. Management of Bottom Ash from WTE Plants – An Overview of Management Options and Treatment Methods. ISWA.

del Valle-Zermeño, R., Gómez-Manrique, J., Giro-Paloma, J., Formosa, J., Chimenos, J. M., 2017. Material characterization of the MSWI bottom ash as a function of particle size. Effects of glass recycling over time. Sci. Total Environ. 581–582, 897–905.

Dzombak, D.A., Morel, F.M., 1991. Surface complexation modeling: hydrous ferric oxide. John Wiley & Sons.

Fischer, H., Meyer, A., Fischer, K., Kuzyakov, Y., 2007. Carbohydrate and amino acid composition of dissolved organic matter leached from soil. Soil Biol. Biochem. 39, 2926–2935.

Flemish-Government 2012. VLAREMA - 17 FEBRUARY 2012. – Order of the Government of Flanders adopting the Flemish regulation on the sustainable management of material cycles and waste. Flanders, Belgium.

Forteza, R., Far, M., Seguí, C., Cerdá, V., 2004. Characterization of bottom ash in municipal solid waste incinerators for its use in road base. Waste Manage. 24, 899–909.

Freire, M., Lopes, H., Tarelho, L.A.C., 2015. Critical aspects of biomass ashes utilization in soils: composition, leachability, PAH and PCDD/F. Waste Manage. 46, 304–315.

French-Republic 2011. Arrêté du 18 novembre 2011 relatif au recyclage en technique routière des mâchefers d'incinération de déchets non dangereux. France.

Funari, V., Gomes, H.I., Cappelletti, M., Fedi, S., Dinelli, E., Rogerson, M., Mayes, W.M., Rovere, M., 2019. Optimization routes for the bioleaching of MSWI fly and bottom ashes using microorganisms collected from a natural system. Waste Biomass Valoriz. 10, 3833–3842.

Geoengineer.org. *Step-by-Step Guide for Grain Size Analysis* [Online]. Geoengineer.org. Available: https://www.geoengineer.org/education/laboratory-testing/step-by-step-guide-for-grain-size-analysis [Accessed January 2023].

Government-of-Wallonia 2001 (last modified in 2018). Arrêté du Gouvernement wallon. Wallonia, Belgium.
HA 2022. Manual of Contract Documents for Highway Works (MCHW). UK.
Head, K.H., 1980. Manual of Soil Laboratory Testing: Soil Classification and Compaction Tests. Wiley.
Holm, O., Simon, F.-G., 2017. Innovative treatment trains of bottom ash (BA) from municipal solid waste incineration (MSWI) in Germany. Waste Manage. 59, 229–236.
Huber, F., Blasenbauer, D., Aschenbrenner, P., Fellner, J., 2020. Complete determination of the material composition of municipal solid waste incineration bottom ash. Waste Manage. 102, 677–685.
Inskeep, W.P., Baham, J., 1983. Competitive complexation of Cd(II) and Cu(II) by water-soluble organic ligands and na-montmorillonite. Soil Sci. Soc. Am. J. 47, 1109–1115.
ISO 2017. 14688-2:2017 Geotechnical investigation and testing. Identification and classification of soil. Part 2: Principles for a classification. Geneva, Switzerland.
Italian-Republic 1998. Decreto 5 febbraio 1998 - (Supplemento ordinario alla Gazzetta ufficiale 16 aprile 1998 n. 88) Individuazione dei rifiuti non pericolosi sottoposti alle procedure semplificate di recupero ai sensi degli articoli 31 e 33 del decreto legislativo 5 febbraio 1997, n. 22 (versione coordinata con il DM 5 aprile 2006). Italy.
Italian-Republic 2006. Decreto 5 aprile 2006, n. 186. Regolamento recante modifiche al decreto ministeriale 5 febbraio 1998 "Individuazione dei rifiuti non pericolosi sottoposti alle procedure semplificate di recupero, ai sensi degli articoli 31 e 33 del decreto legislativo 5 ebbraio 1997, n. 22" (Regulatory that modified Ministerial Decree dated 5 February 1998). Italy: Official Gazette n. 115.
Jadhav, U.U., Biswal, B.K., Chen, Z., Yang, E.-H., Hocheng, H., 2018. Leaching of Metals from incineration bottom ash using organic acid. J. Sustain. Metall. 4, 115–125.
Jang, J.-H., Dempsey, B.A., Burgos, W.D., 2007. Solubility of hematite revisited: effects of hydration. Environ. Sci. Tech. 41, 7303–7308.
Johnson, C.A., Kaeppeli, M., Brandenberger, S., Ulrich, A., Baumann, W., 1999. Hydrological and geochemical factors affecting leachate composition in municipal solid waste incinerator bottom ash: part II. The geochemistry of leachate from Landfill Lostorf, Switzerland. J. Contam. Hydrol. 40, 239–259.
Kannepalli, S., Strom, P.F., Krogmann, U., Subroy, V., Giménez, D., Miskewitz, R., 2016. Characterization of wood mulch and leachate/runoff from three wood recycling facilities. J. Environ. Manage. 182, 421–428.
Kaza, S., Yao, L., Bhada-Tata, P., Woerden, F.V., 2018. What a Waste 2.0: A Global Snapshot of Solid Waste Management to 2050. World Bank, Washington, DC.
Khan, A.A., de Jong, W., Jansens, P.J., Spliethoff, H., 2009. Biomass combustion in fluidized bed boilers: potential problems and remedies. Fuel Process. Technol. 90, 21–50.
Kong, Q., Yao, J., Qiu, Z., Shen, D., 2016. Effect of mass proportion of municipal solid waste incinerator bottom ash layer to municipal solid waste layer on the Cu and Zn discharge from landfill. Biomed Res. Int. 2016, 9687879.
Kosson, D.S., Garrabrants, A., Thorneloe, S., Fagnant, D., Helms, G., Connolly, K., Rodgers, M., 2017. Leaching Environmental Assessment Framework (LEAF). How-To Guide, USA.
Kuzyakov, Y., Leinweber, P., Sapronov, D., Eckhardt, K.-U., 2003. Qualitative assessment of rhizodeposits in non-sterile soil by analytical pyrolysis. J. Plant Nutr. Soil Sci. 166, 719–723.
Laga, 1995a. Anforderungen an die stoffliche Verwertung von mineralischen Reststoffen/Abfällen -Technische Regeln-. Mitteilungen der Länderarbeitsgemeinschaft Abfall (M20) Länderarbeitsgemeinschaft Abfall. Erich Schmidt Verlag, Berlin.
LAGA 1995b. Merkblatt der Landesarbeitsgemeinschaft Abfall für die Entsorgung von Abfällen aus Verbrennungsanlagen für Siedlungsabfälle. Berlin.
Lam, C.H.K., Ip, A.W.M., Barford, J.P., McKay, G., 2010. Use of incineration MSW ash: a review. Sustainability 2, 1943–1968.
Langmuir, D. 1997. Aqueous environmental geochemistry *Prentice Hall: Upper Saddle River, NJ,* 600.
Lederer, J., Syc, M., Biganzoli, L., Bogush, A., Bontempi, E., Braga, R., Costa, G., Funari, V., Grosso, M., Hyks, J., Kameníková, P., Quina, M. M. J., Rasmussen, E., Schlumberger, S., Simon, F. G. & Weibel, G. 2018. Recovery technologies for waste incineration residues (MINEA Deliverable). Mining the European Antroposphere (MINEA).
Lewin, K., Turrell, J., Benson, V., Petrolati, A., 2012. Assessment of Hazard Classification of UK IBA. Swindon, UK.
Lithuanian-Government 2016. ĮSAKYMAS - del atliekų deginimo įrenginiuose ir bendro atliekų deginimo įrenginiuose susidariusių pelenų ir šlako tvarkymo reikalavimų patvirtinimo - 2016 m. lapkričio 25 d. Nr. D1-805,. Vilnius, Lithuania.
LLNL Geochemical Databases and Modeling Codes. California, USA: Lawrence Livermore National Laboratory.
Lockwood, C.L., Mortimer, R.J.G., Stewart, D.I., Mayes, W.M., Peacock, C.L., Polya, D.A., Lythgoe, P.R., Lehoux, A.P., Gruiz, K., Burke, I.T., 2014. Mobilisation of arsenic from bauxite residue (red mud) affected soils: effect of pH and redox conditions. Appl. Geochem. 51, 268–277.
Loginova, E., Volkov, D.S., van de Wouw, P.M.F., Florea, M.V.A., Brouwers, H.J.H., 2019. Detailed characterization of particle size fractions of municipal solid waste incineration bottom ash. J. Clean. Prod. 207, 866–874.
Lu, H., Sun, J., Zhu, L., 2017. The role of artificial root exudate components in facilitating the degradation of pyrene in soil. Sci. Rep. 7, 7130.
Mantovani, L., De Matteis, C., Tribaudino, M., Boschetti, T., Funari, V., Dinelli, E., Toller, S., Pelagatti, P., 2023. Grain size and mineralogical constraints on leaching in the bottom ashes from municipal solid waste incineration: a comparison of five plants in northern Italy. Front. Environ. Sci. 11.
Meima, J.A., Comans, R.N.J., 1997. Geochemical modeling of weathering reactions in municipal solid waste incinerator bottom ash. Environ. Sci. Tech. 31, 1269–1276.
Meima, J.A., van Zomeren, A., Comans, R.N.J., 1999. Complexation of Cu with dissolved organic carbon in municipal solid waste incinerator bottom ash leachates. Environ. Sci. Tech. 33, 1424–1429.
Millward, G.E., Moore, R.M., 1982. The adsorption of Cu, Mn and Zn by iron oxyhydroxide in model estuarine solutions. Water Res. 16, 981–985.
Mirsayar, M.M., Joneidi, V.A., Petrescu, R.V.V., Petrescu, F.I.T., Berto, F., 2017. Extended MTSN criterion for fracture analysis of soda lime glass. Eng. Fract. Mech. 178, 50–59.
Morf, L.S., Brunner, P.H., Spaun, S., 2000. Effect of operating conditions and input variations on the partitioning of metals in a municipal solid waste incinerator. Waste Manage. Res. 18, 4–15.
Murray, H. H. 2006. Chapter 5 Kaolin Applications. *In:* MURRAY, H. H. (ed.) *Developments in Clay Science.* Elsevier.
Myneni, S.C.B., Traina, S.J., Logan, T.J., 1998. Ettringite solubility and geochemistry of the Ca(OH)2–Al2(SO4), 3–H2O system at 1 atm pressure and 298 K. Chem. Geol. 148, 1–19.
Olsson, S., van Schaik, J.W.J., Gustafsson, J.P., Kleja, D.B., van Hees, P.A.W., 2007. Copper(II) binding to dissolved organic matter fractions in municipal solid waste incinerator bottom ash leachate. Environ. Sci. Tech. 41, 4286–4291.
Parkhurst, D.L., Appelo, C., 2013. Description of input and examples for PHREEQC version 3—a computer program for speciation, batch-reaction, one-dimensional transport, and inverse geochemical calculations. US Geol. Surv. Tech. Methods 6, 497.
Peng, N., Li, Y., Liu, Z., Liu, T., Gai, C., 2016. Emission, distribution and toxicity of polycyclic aromatic hydrocarbons (PAHs) during municipal solid waste (MSW) and coal co-combustion. Sci. Total Environ. 565, 1201–1207.
Ravel, B., Newville, M., 2005. ATHENA, ARTEMIS, HEPHAESTUS: data analysis for X-ray absorption spectroscopy using IFEFFIT. J. Synchrotron Radiat. 12, 537–541.
Republic-of-Austria 2017a. Bundesabfallwirtschaftsplan 2017 - Teil 1 (Federal Waste Management Plan 2017). Austria.
Republic-of-Austria 2017b. Technische Grundlagen für den Einsatz von Abfällen als Ersatzrohstoffe in Anlagen zur Zementerzeugung (English: Technical basics for the use of waste as secondary raw material in cement production.). Austria.
RIVM 2007. Regeling van 13 december 2007, nr. DJZ2007124397, houdende regels voor de uitvoering van de kwaliteit van de bodem. Bilthoven, Netherlands: Rijkswaterstaat, Rijksinstituut voor Volksgezondheid en Milieu.
Shah, A.V., Srivastava, V.K., Mohanty, S.S., Varjani, S., 2021. Municipal solid waste as a sustainable resource for energy production: state-of-the-art review. J. Environ. Chem. Eng. 9, 105717.
Sjöberg, E.L., Rickard, D.T., 1984. Temperature dependence of calcite dissolution kinetics between 1 and 62 °C at pH 2.7 to 8.4 in aqueous solutions. Geochim. Cosmochim. Acta 48, 485–493.
Smith, L., Sutherland, N. & Bolton, P. 2022. Commons Library debate pack: Permit variation processes for waste incineration facilities House of Commons Library.
Speiser, C., Baumann, T., Niessner, R., 2001. Characterization of municipal solid waste incineration (MSWI) bottom ash by scanning electron microscopy and quantitative energy dispersive X-ray microanalysis (SEM/EDX). Fresenius J. Anal. Chem. 370, 752–759.
Strohmeier, S., Knorr, K.H., Reichert, M., Frei, S., Fleckenstein, J.H., Peiffer, S., Matzner, E., 2013. Concentrations and fluxes of dissolved organic carbon in runoff from a forested catchment: insights from high frequency measurements. Biogeosciences 10, 905–916.
Suez. *Energy-from-waste: How does energy-from-waste work?* [Online]. suez.co.uk. Available: https://www.suez.co.uk/en-gb/our-offering/communities-and-individuals/education-tools-and-resources/what-happens-to-waste/general-waste/energy-from-waste#:~:text=Inside%20the%20furnace%2C%20a%20series,can%20be%20used%20in%20construction. [Accessed 2024].
Swedish-EPA, 2010. Recycling of Waste in Facility Works. Återvinning av avfall i anläggningsarbeten, Handbok. Swedish EPA document, In Swedish.
Swedish-EPA,, 2011. Low POP Content Limit OF PCDD/F in Waste. Swedish Environmental Protection Agency, Evaluation of human health risks Stockholm.
Šyc, M., Simon, F.G., Hykš, J., Braga, R., Biganzoli, L., Costa, G., Funari, V., Grosso, M., 2020. Metal recovery from incineration bottom ash: state-of-the-art and recent developments. J. Hazard. Mater. 393, 122433.
Tao, W., Hall, K.J., Masbough, A., Frankowski, K., Duff, S.J.B., 2005. Characterization of leachate from a woodwaste pile. Water Qual. Res. J. 40, 476–483.
Taylor, B.R., Carmichael, N.B., 2003. Toxicity and chemistry of aspen wood leachate to aquatic life: field study. Environ. Toxicol. Chem. 22, 2048–2056.
Tolvik,, 2022. UK Energy from Waste Statistics – 2021. Tolvik Consulting, UK.
UKEA, 2009. Incineration of Waste (EPR5.01): Additional Guidance. How to Comply with Your Environmental Permit: Technical Guidance for Operators. Environment Agency, Bristol.
UKEA, 2021. Waste Classification: Guidance on the Classification and Assessment of Waste. UK.
UKEA 2023. Using unbound incinerator bottom ash aggregate (IBAA) in construction activities: RPS 247. England.
UNEP, 2001. The Stockholm Convention on Persistent Organic Pollutants. UN Environment Programme, Stockholm.
USEPA 1994. Method 1613: Tetra-Through Octa-Chlorinated Dioxins and Furans by Isotope Dilution HRGC/HRMS. Washington, D.C.: Office of Water Engineering and Analysis Division, United States Environmental Protection Agency.
USEPA 2010. Method 1668C Chlorinated Biphenyl Congeners in Water, Soil, Sediment, Biosolids, and Tissue by HRGC/HRMS Washington, DC: Office of Water, Office of

Science and Technology, Engineering and Analysis Division, United States Environmental Protection Agency.
USEPA 2017. Method 1313: Liquid-Solid Partitioning as a Function of Extract pH Using a Parallel Batch Extraction Procedure Washington, DC: Office of Land and Environmental Management, United States Environmental Protection Agency.
Valorsul 2017. Relatorío & Contas. Portugal.
van den Berg, M. J. A. & West, N. 1997. Chapter 12: Standardization of leaching/extraction tests. *In:* VAN DER SLEET, H. A., HEASMAN, L. & QUEVAUVILLER, P. (eds.) *Studies in Environmental Science.* Elsevier.
Van Gerven, T., Geysen, D., Stoffels, L., Jaspers, M., Wauters, G., Vandecasteele, C., 2005. Management of incinerator residues in Flanders (Belgium) and in neighbouring countries. A Comparison. Waste Manage. 25, 75–87.
van Hees, P.A.W., Jones, D.L., Finlay, R., Godbold, D.L., Lundström, U.S., 2005. The carbon we do not see—the impact of low molecular weight compounds on carbon dynamics and respiration in forest soils: a review. Soil Biol. Biochem. 37, 1–13.
Vehmaanperä, P. 2022. *Dissolution of magnetite and hematite in acid mixtures.* Dissertation for the degree of Doctor of Science (Technology), Lappeenranta-Lahti University of Technology LUT.
Violante, A. 2013. Chapter Three - Elucidating Mechanisms of Competitive Sorption at the Mineral/Water Interface. *In:* SPARKS, D. L. (ed.) *Advances in Agronomy.* Academic Press.
Wang, X., Dai, Z., Zhao, Y., Dai, C., Ko, S., Paudyal, S., Yao, X., Leschied, C., Kan, A. T. & Tomson, M. B. Zinc Sulfide Solubility Modeling in Aqueous Solution at High Temperature, Pressure, and Ionic Strength. AMPP Annual Conference + Expo, 2022. D021S006R005.
Wei, Y., Shimaoka, T., Saffarzadeh, A., Takahashi, F., 2011. Mineralogical characterization of municipal solid waste incineration bottom ash with an emphasis on heavy metal-bearing phases. J. Hazard. Mater. 187, 534–543.
Weidner, E., Ciesielczyk, F., 2019. Removal of hazardous oxyanions from the environment using metal-oxide-based materials. Materials 12, 927.
Weng, L., Temminghoff, E.J.M., Lofts, S., Tipping, E., Van Riemsdijk, W.H., 2002. Complexation with dissolved organic matter and solubility control of heavy metals in a sandy soil. Environ. Sci. Technol. 36, 4804–4810.
Worrall, F., Harriman, R., Evans, C.D., Watts, C.D., Adamson, J., Neal, C., Tipping, E., Burt, T., Grieve, I., Monteith, D., Naden, P.S., Nisbet, T., Reynolds, B., Stevens, P., 2004. Trends in dissolved organic carbon in UK rivers and lakes. Biogeochemistry 70, 369–402.
Yan, Y., Wan, B., Mansor, M., Wang, X., Zhang, Q., Kappler, A., Feng, X., 2022. Co-sorption of metal ions and inorganic anions/organic ligands on environmental minerals: a review. Sci. Total Environ. 803, 149918.
Yao, J., Li, W.-B., Kong, Q.-N., Wu, Y.-Y., He, R., Shen, D.-S., 2010. Content, mobility and transfer behavior of heavy metals in MSWI bottom ash in Zhejiang province, China. Fuel 89, 616–622.
Young, C.A., Dahlgren, E.J., Robins, R.G., 2003. The solubility of copper sulfides under reducing conditions. Hydrometall. 68, 23–31.
Yuan, G., Cao, Y., Schulz, H.-M., Hao, F., Gluyas, J., Liu, K., Yang, T., Wang, Y., Xi, K., Li, F., 2019. A review of feldspar alteration and its geological significance in sedimentary basins: from shallow aquifers to deep hydrocarbon reservoirs. Earth Sci. Rev. 191, 114–140.
Zhang, D.Q., Tan, S.K., Gersberg, R.M., 2010. Municipal solid waste management in China: status, problems and challenges. J. Environ. Manage. 91, 1623–1633.
Zhu, Y., Zhao, Y., Zhao, C., Gupta, R., 2020. Physicochemical characterization and heavy metals leaching potential of municipal solid waste incinerated bottom ash (MSWI-BA) when utilized in road construction. Environ. Sci. Pollut. Res. 27, 14184–14197.